

# **Supplementary Material**

**accompanying the manuscript**

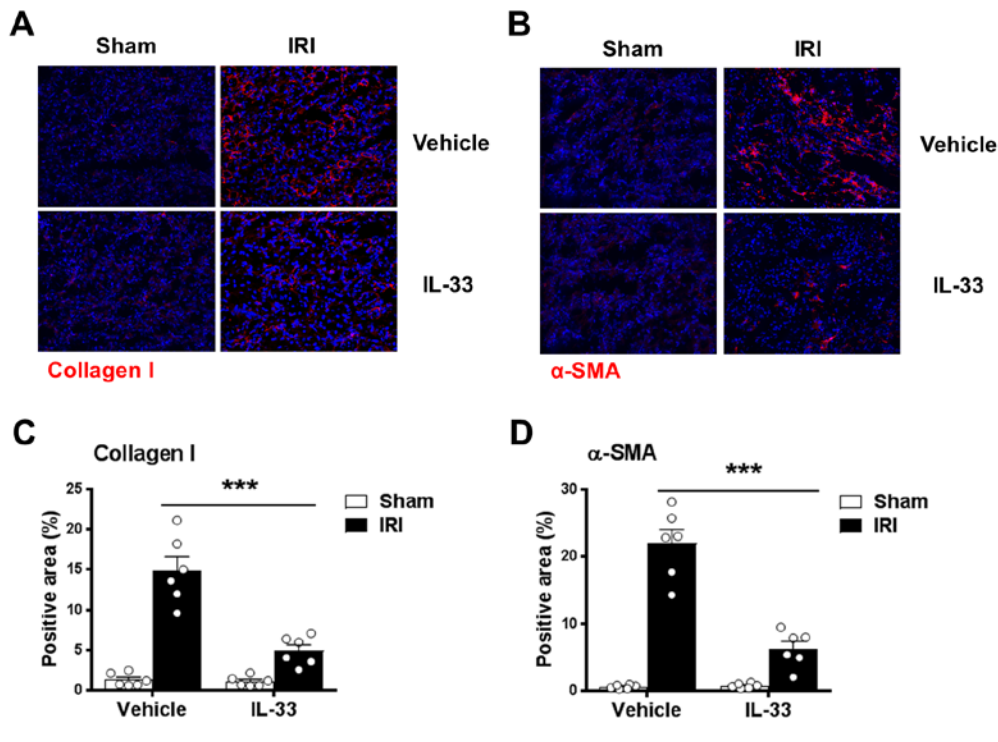
**Potentiating tissue resident type 2 innate lymphoid cells by IL-33 to prevent renal ischemia/reperfusion injury**

Qi Cao, Yiping Wang, Zhiguo Niu, Chengshi Wang, Ruifeng Wang, Zhiqiang Zhang, Titi Chen, Xin Maggie Wang, Qing Li, Vincent W.S. Lee, Qingsong Huang, Jing Tan, Minghao Guo, Yuan Min Wang, Guoping Zheng, Di Yu, Stephen I. Alexander, Hui Wang and David C.H. Harris

**This PDF file includes:**

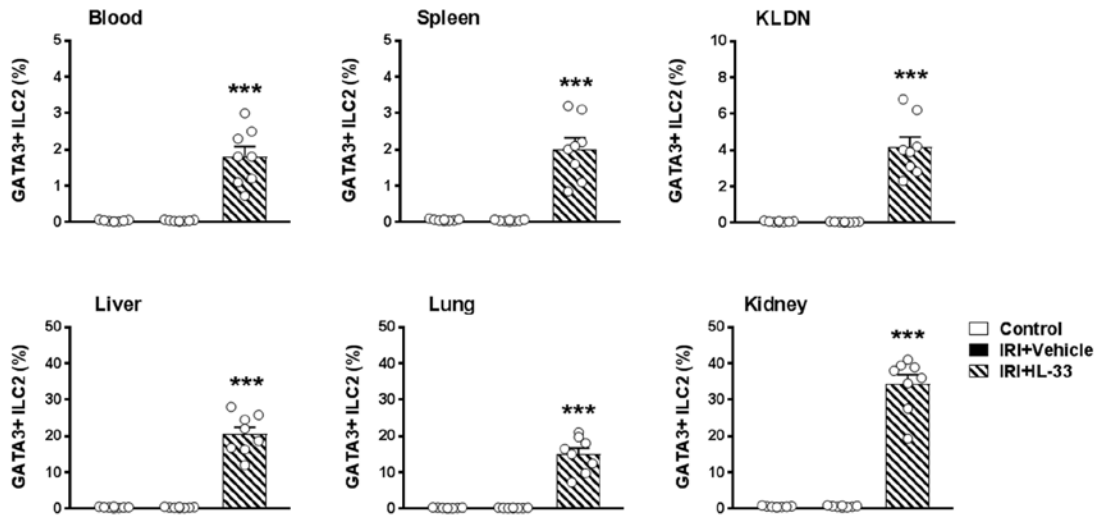
Figures S1 to S7.

Table S1.



**Figure S1. IL-33 reduced renal fibrosis in IRI mice.**

C57BL/6 mice were treated with mouse recombinant IL-33 daily for 5 consecutive days before unilateral IRI. Mice were euthanized at day 28 after IRI. (A, B) Immunostaining of collagen I (red) and  $\alpha$ -SMA (red) in sham and postischemic kidneys of unilateral IRI mice treated with PBS or IL-33. (C, D) The percentage of total tissue area that stained positively for collagen I and  $\alpha$ -SMA in sham and postischemic kidneys at 28 days after IRI. Data shown are the mean  $\pm$  SEM (n=6 per group); \*\*\*P<0.001 vs. Vehicle.



**Figure S2. IL-33 induced ILC2 in multiple anatomical sites of IRI mice.**

C57BL/6 mice were treated with mouse recombinant IL-33 daily for 5 consecutive days before IRI. Indicated tissues were harvested at day one after IRI, and the frequency of GATA3+ ILC2 in the CD45+ leukocyte compartment from blood, spleen, kidney draining lymph node (KLDN), liver, lung and kidney were assessed by flow cytometry in control, IRI+Vehicle or IRI+IL-33 mice. Data shown are the mean  $\pm$  SEM (n=8 per group); \*\*\*P<0.001 vs. control, IRI+vehicle.

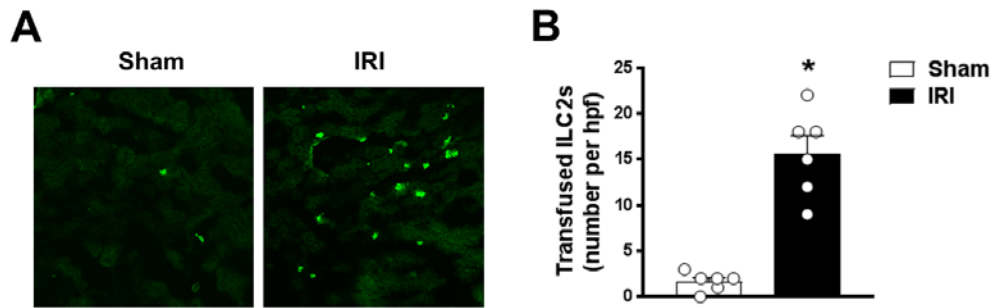


**Figure S3. Transfused mouse ILC2 distributed into kidney.**

CFSE labeled ILC2 cells were adoptively transferred into Rag<sup>-/-</sup> mice one day before unilateral IRI. (A) Transfused CFSE<sup>+</sup> ILC2s were observed in sham kidney and IRI kidney at day one after IRI. (B) Numbers of CFSE labeled ILC2 cells in sham kidney and IRI kidney were counted. Data shown are the mean  $\pm$  SEM per high power field (hpf) from each group (n=6 per group).

\*P<0.05 vs. Sham.

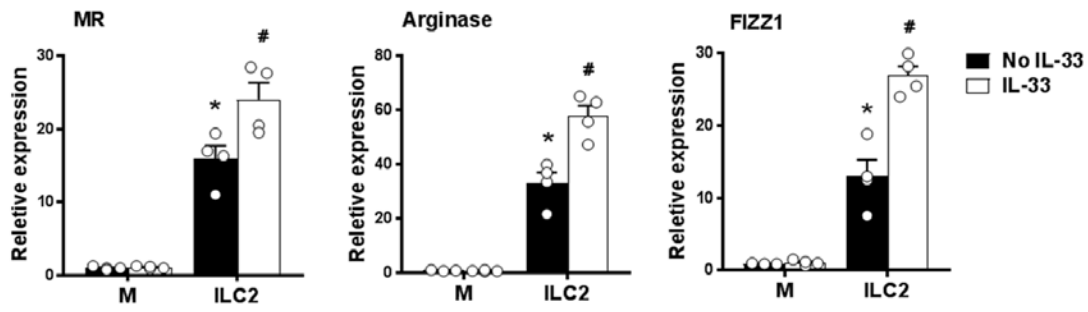


**Figure S4. ILC2 induce M2 macrophages in vitro.**

Bone marrow macrophages were preincubated with or without mouse recombinant IL-33 for 1 hour and then cultured with complete medium (M) or ILC2 for 6 hours. Macrophage phenotype was examined by qPCR. The mRNA expression of M2 macrophage markers (MR, arginase and FIZZ1) was examined by qPCR in bone marrow macrophages. Data are representative of three independent experiments. \* $P < 0.05$  vs. M, # $P < 0.05$  vs. No IL-33.

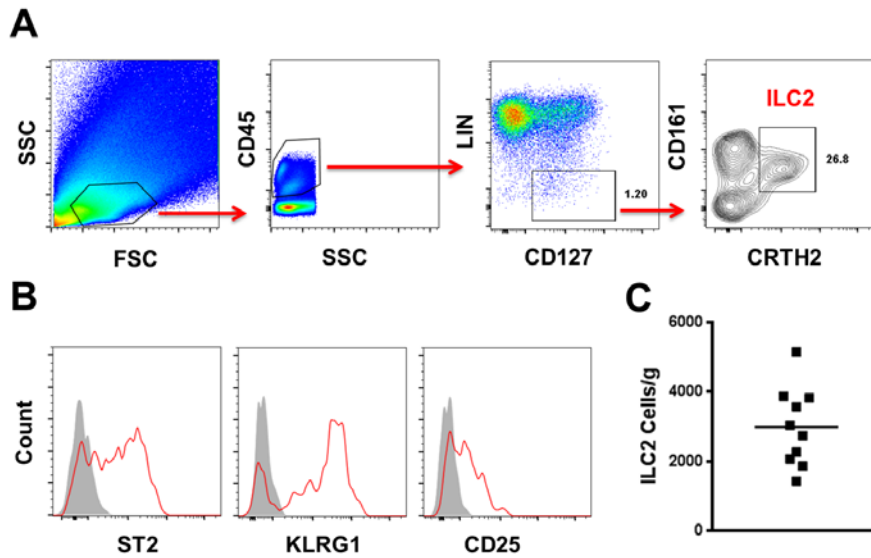


**Figure S5. Identification of ILC2 in human kidney tissue.**

Renal cortical tissue was obtained with informed patient consent from the healthy portion of tumor or trauma nephrectomy specimens. (A) Representative FACS analysis showing the gating strategy to identify CD45+Lin-CD127+CD161+CRTH2+ ILC2 in human kidney tissue. Lin mixture includes CD3, TCR $\alpha\beta$ , CD19, CD20, CD14, CD16, CD11b, CD11c, CD123, CD56 and Fc $\epsilon$ RI $\alpha$ . (B) Histogram showing expression of ST2, KLRG1 and CD25 on kidney ILC2 cells. Specific markers (red lines) and isotype controls (gray-filled areas) are shown. (C) The absolute number of CD161+CRTH2+ ILC2 in one gram of human kidney tissue (n=10).

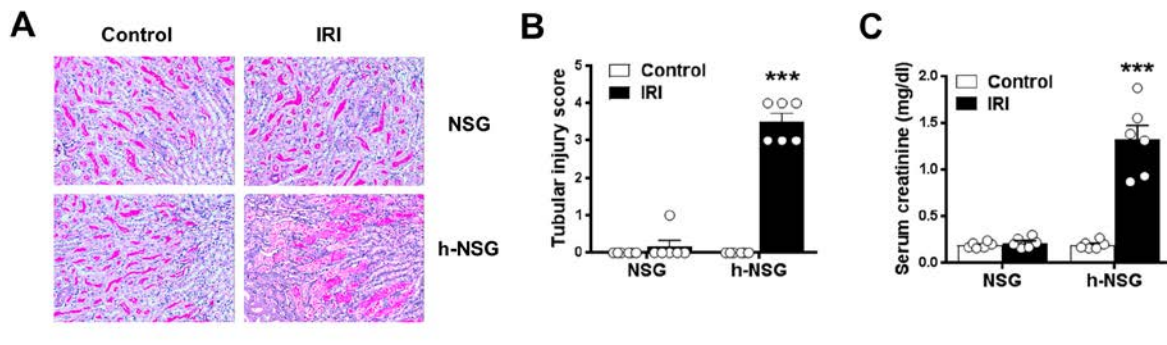


**Figure S6. Human immune cells induced IRI in NSG mice.**

Bilateral IRI was performed for 35 minutes at 37 °C in NSG mice and humanized NSG mice. Animals subjected to sham operation were used as controls. Mice were euthanized one day after IRI. (A) Representative PAS-stained sections of kidney outer medulla from NSG and humanized NSG (h-NSG) mice ( $\times 200$ ). (B, C) Tubular injury score and serum creatinine levels were assessed in mice at one day after IRI. Data shown are the mean  $\pm$  SEM (n=6 per group); \*\*\*P<0.001 vs. IRI+vehicle.

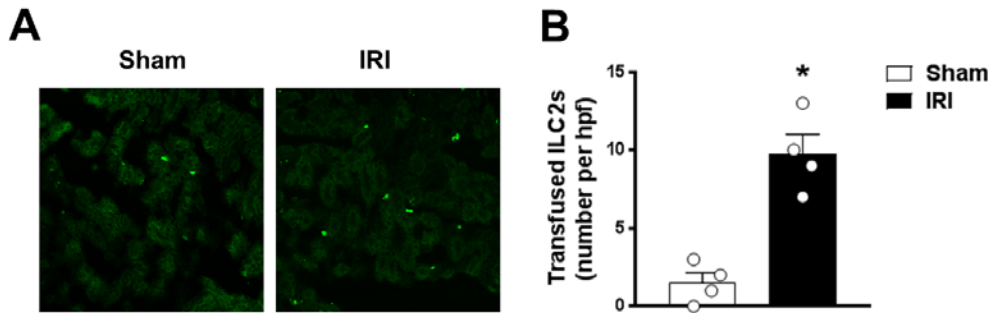


**Figure S7. Transfused human ILC2 distributed into kidney of h-NSG mice.**

CFSE labeled human ILC2 cells were adoptively transferred into humanized NSG (h-NSG) mice one day before unilateral IRI. (A) Transfused CFSE<sup>+</sup> human ILC2s were observed in sham kidney and IRI kidney at day one after IRI. (B) Numbers of CFSE labeled ILC2 cells in sham kidney and IRI kidney were counted. Data shown are the mean  $\pm$  SEM per high power field (hpf) from each group (n=4 per group). \*P<0.05 vs. Sham.



**Table S1.** Real-time PCR primers

<b>Gene</b>	<b>Forward (5'-3')</b>	<b>Reverse (5'-3')</b>
IL-4 (M)	tcaacccccagctagtgtgc	tctgtggtgttcttcgttgc
IL-13 (M)	cagcatggatggagtgtgg	aggctggagaccgtagtgg
Mannose receptor (M)	caaggaaggtggcatttgt	ccttcagtcctttgcaagc
Arginase (M)	agtctggcagttggaagcat	ctggtgtcaggggagtgtt
HO-1 (M)	ggtgatggcttcttgtacc	agtgaggccataaccagaag
FIZZ1 (M)	tgctgggatgactgctactg	ctgggttctccaccttca
IL10 (M)	ccagtacagccgggaagaca	cagctggtcctttgtttgaaaga
iNOS (M)	cacctggagttcaccagt	accactcgtacttgggatgc
TNF- $\alpha$ (M)	gctgagctcaaaccctgta	cggactccgaaagtctaag
IL-1 $\beta$ (M)	tgccacctttgacagtgatg	atgtgctgctgcgagatttg
IL-6 (M)	cacaagtccggagaggagac	ttgccattgcacaactcttt
CCL2 (M)	agcaccagccaactctcact	cgtaactgcatctggctga
CXCL1 (M)	tggtgggattcacctcaagaaca	tgtggctatgacttcggttgggt
CXCL2 (M)	acatcccaccacacagtgaaga	acatcccaccacacagtgaaga
Mannose receptor (H)	cgaggaagaggttcggtcacc	gcaatcccgttctcatggc
CCL18 (H)	agctctgctgcctcgtctat	cccacttctattggggctca
IL-10 (H)	gatccagttttacctggaggag	cctgagggcttccaggttctc
TNF- $\alpha$ (H)	cagagggcctgtacctcatc	ggaagaccctcccagatag
IL-1 $\beta$ (H)	gggcctcaaggaagaatc	ttctgctgagaggtgctga
CCL2 (H)	ccccagtcacctgctgttat	tggaatcctgaaccacttc

M=mouse, H=human.